



Surface reconstruction of the surgical field from stereoscopic microscope views in neurosurgery

Oliver Fleig, Frédéric Devernay, Jean-Marie Scarabin, Pierre Jannin

► To cite this version:

Oliver Fleig, Frédéric Devernay, Jean-Marie Scarabin, Pierre Jannin. Surface reconstruction of the surgical field from stereoscopic microscope views in neurosurgery. *Computer Assisted Radiology and Surgery*, 2001, Berlin, Germany. pp.268-274, 10.1016/S0531-5131(01)00054-1 . hal-00816696

HAL Id: hal-00816696

<https://hal.inria.fr/hal-00816696>

Submitted on 22 Apr 2013

HAL is a multi-disciplinary open access archive for the deposit and dissemination of scientific research documents, whether they are published or not. The documents may come from teaching and research institutions in France or abroad, or from public or private research centers.

L'archive ouverte pluridisciplinaire **HAL**, est destinée au dépôt et à la diffusion de documents scientifiques de niveau recherche, publiés ou non, émanant des établissements d'enseignement et de recherche français ou étrangers, des laboratoires publics ou privés.

Surface reconstruction of the surgical field from stereoscopic microscope views in neurosurgery

O. J. Fleig^{ab*}, F. Devernay^c, J.-M. Scarabin^{ad} and P. Jannin^a

^aLaboratoire SIM, Faculté de Médecine, Université de Rennes 1, 2 Avenue du Pr. Léon Bernard, 35043 Rennes Cedex (France)

^bCarl Zeiss S.A., 60 Route de Sartrouville, 78230 Le Pecq (France)

^cTeam ChIR, INRIA, Sophia-Antipolis (France)

^dDepartment of Neurosurgery, University Hospital of Rennes, (France)

We present a technique to reconstruct the surface of the surgical field during neurosurgery. The images are taken with a stereo camera mounted on a surgical microscope, which is part of a neuronavigation system. We use an intensity-based method to calculate a dense disparity map over the whole image extend. Correspondences are established by exploiting the epipolar geometry and comparing image intensities along corresponding epipolar lines. The method does not require a strong calibration. Only the colineation denoted by the fundamental matrix, which maps corresponding epipolar lines from one image to the other, has to be known. The results show that our method is able to reconstruct the surface of the surgical field upto a few areas. It is limited at points of specular reflections of the wet brain surface and points of uniform texture.

Keywords: Stereoscopic reconstruction; neuronavigation; stereo microscope; augmented reality; augmented virtuality

1. Introduction

In neurosurgery, guidance systems, which correlate patient imaging data to the surgical field using tracked probes or surgical microscopes, have become standard equipment. The most advanced systems dispose of an additional head-up display showing relevant information on a two-dimensional graphical overlay directly within one of the oculars of the microscope. Our experience has shown that to take full advantage of augmented reality, more complex colour and stereoscopic displays are needed for a better understanding and interpretation of the overlaid information [1]. Therefore, this basic overlay will be replaced in future by more sophisticated three-dimensional displays being able to render stereoscopic views of a virtual scene. Today's augmented reality, where the real scene's information is enhanced with additional information, might be backed by augmented virtuality [2,3]. Augmented virtuality fuses multimodal scene information acquired during planning with real-time images from the surgical field. To ade-

*Contact: Oliver.Fleig@univ-rennes1.fr <http://sim3.univ-rennes1.fr>

quately merge real and virtual information for both augmented reality and virtuality we need to know surface information on the real scene. E.g. to determine which part of a virtual object would be occluded by the real scene, we need to know the surface of the surgical field.

With the surgical microscope we dispose of the possibility to record corresponding stereo images from the right and left ocular, without expensive additional hardware.

AUDETTE proposes in his work on brain deformation [4] the use of a commercial range-sensor and structured laser light to reconstruct the brain surface. SKRINJAR uses a strongly calibrated stereo rig and an integration technique to compute the surface normals from the partial derivatives of intensities in both images [5]. Integration techniques accumulate errors and constrain the surface to be continuous and globally follow the Lambertian reflectance model.

We also use an intensity-based method, where point correspondences are established by comparing intensities within a defined window in the left and right image [6]. This method works on surfaces which are only *locally* Lambertian and may contain discontinuities in the disparity. Intensity-based methods calculate dense disparity maps in opposition to feature based methods, which recover only sparse disparity maps.

2. Material and Methods

2.1. Acquisition

The Department of Neurosurgery at the University Hospital of Rennes disposes of an SMN zoom lens microscope from CARL ZEISS (Oberkochen, Germany). A localiser tracks patient, probe, and microscope position. A pair of stereoscopic single CCD cameras mounted on the microscope is used to record still colour images with an off-the-shelf video grabber card on a desktop PC. A video channel switch driven by the parallel port of the PC selects between the left and right ocular. Focus and zoom parameters as well as the tracked microscope position are transferred from the navigation system to the PC via serial port connection. A simple user interface under MS-Windows initiates grabbing of an image pair and stores it along with zoom and focus settings and the microscope position.

2.2. Epipolar geometry and fundamental matrix

To reconstruct the surface from two images, point correspondences have to be established. We take advantage of the epipolar geometry to simplify the search for corresponding points [6,7]. The epipolar geometry constraints points lying on an epipolar line in the left image to be projected onto the corresponding epipolar line in the right image. The fundamental matrix is a colineation that gives the correspondence between epipolar lines, and allows to establish the equation of the epipolar line in the right image corresponding to a point given in the left image. To find a match to a point from the left image, the search is limited to the corresponding epipolar line in the right image. The fundamental matrix is calculated from one or multiple pairs of images with the same settings for zoom and focus. To minimise numerical instability we used multiple views at the same settings by generating additional sets of images of a calibration grid. The colineation between lines in the right and left images described by the fundamental matrix has seven degrees of freedom and can be solved using least square method based on at least eight pairs of corresponding points [8]. Points are extracted automatically using curvature operators and matches are automatically established using a relaxation based algorithm.

2.3. Rectification

To simplify point comparisons the fundamental matrix is used to rectify the image pairs in the way that corresponding epipolar lines are parallel to the abscissa at the same value for the ordinate in the image coordinate system [7,9]. Figure 1 shows the rectified image of the left ocular.

2.4. Disparity map

After rectification for each point of the left images, a corresponding point has to be found on the epipolar with the same ordinate value. The luminance within a window of predefined size is compared using a *zero-mean normalised sum of squared differences* (ZNSSD) criterion:

$$ZNSSD_{x,y}(d) = -\frac{\sum_{i,j}(I'_l(x+i, y+j) - I'_r(x+i+d, y+j))^2}{\sqrt{\sum_{i,j}\bar{I}_r(x+i+d, y+j)^2}}$$

where d denotes the disparity and $I' = I(x, y) - \bar{I}(x, y)$, with $I(x, y)$ for the intensity at image point (x, y) and $\bar{I}(x, y)$ for the mean intensity over the correlation window of size $(2w+1) \times (2h+1)$. Indices l and r denote the left and right images respectively. For the sums we have $-w \leq i \leq w$ and $-h \leq j \leq h$ with $i, j \in \mathbb{Z}$.

If the criterion is below a defined threshold the point pair is a match candidate. The difference in the abscissa value of two match candidates is called disparity. Additional robustness for the point pairing is achieved by respecting the ordering constraint, which says that the ordering of corresponding points remains unchanged on corresponding epipolar lines. The search interval for the disparity is determined by the optical geometry of the microscope and the cameras, and the position of the surface relative to the microscope.

A subsequently applied median filter and an erosion remove false positives from the disparity map. A further filter computes the derivatives of the disparity map and smoothes it by locally fitting a plane to the points in the filter window [10]. Figures 2 and 3 show the disparity maps before and after filtering.

2.5. Reconstruction

The surface can be directly reconstructed from the disparity map: larger disparities correspond to points closer to the observer. The reconstruction based on an estimated fundamental matrix can only be determined up to a projective transformation. From the calibration of the microscope and the fundamental matrix this final projective transformation matrix can be calculated [11]. Figure 4 shows an example of a reconstructed surface.

3. Results

Until now we have been able to apply the method on intra-operative images of four patients and a total of twenty image pairs. The extend of the observed fields of view reached from about 7 cm to 12 cm. The image resolution is 768×576 pixels. For each set of zoom and focus setting calibration images have been taken right after the operation to prevent errors from camera fixation. The errors for the calculation of the fundamental matrix are in the order of one pixel. A window size of 11 pixels gives the best results for our preliminary tests for luminance matching followed by a smoothing step on the disparity map with a 7 pixel window size. The search interval for the disparity map is adjusted manually by comparing points of interest in

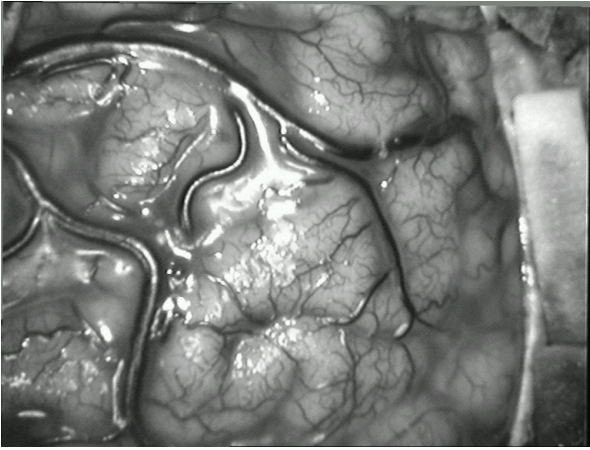


Figure 1. Rectified image of the left microscope view.

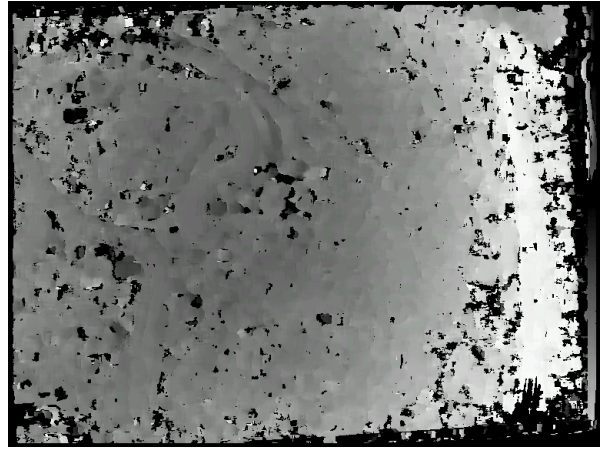


Figure 2. Disparity map from ZNSSD criterion.

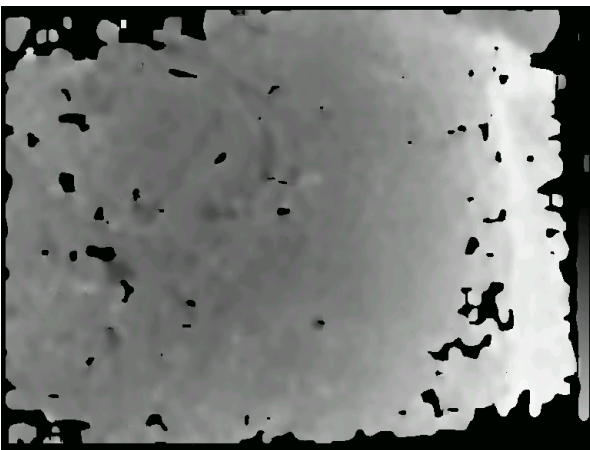


Figure 3. Disparity map after median filtering and local plane fitting.

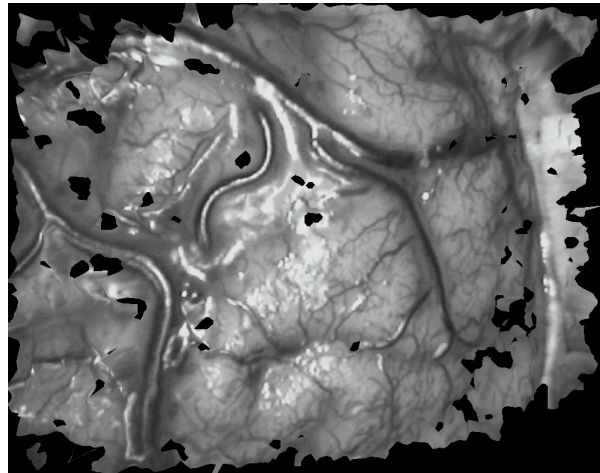


Figure 4. Reconstructed surface, textured-mapped with the original image. The holes correspond to the areas where the disparity map contains no information.

the image pairs. Overall calculation of the disparity map performs very good. However, the matching fails on various regions and points in the images and leaves multiple holes in the disparity map.

Examination of the regions which were not reconstructed shows that most of them are saturated in one or both of the original images due to specular reflection. Other regions which were not reconstructed are areas on the border of the surgical field with gauze or cloth where there is no texture to exploit for the luminance comparison. Although the brain surface is speckled with tiny vessels which give it enough texture for reconstruction there are some areas on larger gyri of uniform colour. Those areas are not recovered by the reconstruction either.

4. Discussion and Conclusion

We have demonstrated that the stereoscopic reconstruction of the brain is feasible from only the two images of a stereoscopic microscope view. The main problem is the particularity of the intra-operative images of the brain surface. The microscope's light source is parallel to the optical axes which, in conjunction with the wet brain surface, causes a large amount of specular reflection. We cannot calculate the surface by luminance comparison for pixels in these reflection areas. But the results are still satisfactory as we do not need to know the exact surface of every point. For visual application like the already mentioned occlusion problem it seems sufficient to fill the holes in the disparity map with an interpolation technique by exploiting an a priori knowledge about the surface. Such an a priori knowledge is the fact that the reconstructed surface is a single surface and relatively smooth.

For other applications like distance measures for brain-shift evaluation it is preferable not to interpolate, since the accuracy of the reconstructed points is more important than the number of these points.

The authors are aware of the fact that validation is of immediate concern for the further use of this method. To validate the accuracy of the reconstruction, we plan to apply the algorithm on known synthetic scene with real intra-operative images as object texture. The microscope calibration has to be recovered in order to pass from the for the moment only projective reconstruction to an euclidian reconstruction.

We also have to evaluate the reconstruction of images at a higher magnification. At a higher magnification we might probably loose some texture from the vessels and have larger areas of unrecoverable uniform intensity.

We consider intra-operative stereoscopic images from the surgical microscope as a sofar unexploited additional modality in multimodal neurosurgery. We already mentioned brain-shift estimation and occlusion as possible applications. A surface reconstruction gives us also the possibility to update a scene depending on the progress of the intervention or to verify or establish registration to the patient. There is also the possibility to calculate the volume of resection.

Our method does not require expensive additional equipment as long as it is possible to capture intra-operative images from a surgical microscope.

REFERENCES

1. Pierre Jannin, Oliver J. Fleig, Eric Seigneuret, Christophe Grova, Xavier Morandi, and Jean-Marie Scarabin. A data fusion environment for multimodal and multi-informational neuronavigation. *Computer Aided Surgery*, 5:1–10, 2000.

2. Damini Dey, Piotr J. Slomka, David G. Gobbi, and Terry M. Peters. Mixed Reality Merging of Endoscopic Images and 3-D Surfaces. In *Medical Image Computing and Computer-Assisted Intervention (MICCAI)*, volume 1935 of *Lecture Notes in Computer Science*, pages 796–803. Springer Verlag, 2000.
3. P. Jannin, A. Bouliou, E. Journet, and J. M. Scarabin. Ray-traced texture mapping for enhanced virtuality in image-guided neurosurgery. In *Stud Health Technol Inform*, volume 29, pages 553–563, 1996.
4. M.A. Audette, K. Siddiqi, and T.M. Peter. Level-set surface segmentation and fast cortical range image tracking for computing intrasurgical deformations. In *Medical Image Computing and Computer-Assisted Intervention (MICCAI)*, volume 1679 of *Lecture Notes in Computer Science*, pages 788–797. Springer Verlag, 1999.
5. Oskar Skrinjar, Hemant Tagare, and James Duncan. Surface growing from stereo images. In *IEEE Computer Society Conference on Computer Vision and Pattern Recognition (CVPR 2000)*, volume II, pages 571–576, Hilton Head Island, SC, USA, june 2000.
6. R. Klette, K Schüns, and A Koschan. *Computer Vision: Three-Dimensional Data from Images*. Springer, 1998.
7. Olivier Faugeras. *Three-Dimensional Computer Vision: A Geometric Viewpoint*. MIT Press, Cambridge, Massachusetts, 1993.
8. Zhengyou Zhang, Rachid Deriche, Olivier Faugeras, and Q. T. Luong. A robust technique for matching two uncalibrated images through the recovery of the unknown epipolar geometry. Technical Report RR-2273, Inria, Institut National de Recherche en Informatique et en Automatique, 1994.
9. N. Ayache. *Artificial Vision for Mobile Robots: Stereo Vision and Multi-sensory Perception*. MIT Press, Cambridge, MA, 1991.
10. Frédéric Devernay and O. D. Faugeras. Computing differential properties of 3-D shapes from stereoscopic images without 3-D models. In *Proceedings of the International Conference on Computer Vision and Pattern Recognition*, pages 208–213, 1994.
11. Frederic Devernay and Olivier Faugeras. From projective to euclidean reconstruction. In *Proceedings of the International Conference on Computer Vision and Pattern Recognition*, pages 264–269, 1996.